



Title	Nature of red luminescence band in research-grade ZnO single crystals: A “self-activated” configurational transition
Author(s)	CHEN, YN; Xu, S; Zheng, C; Ning, J; Ling, FCC; Anwand, W; Brauer, G; Skorupa, W
Citation	Applied Physics Letters, 2014, v. 105 n. 4, p. 041912
Issued Date	2014
URL	http://hdl.handle.net/10722/200813
Rights	Creative Commons: Attribution 3.0 Hong Kong License

Nature of red luminescence band in research-grade ZnO single crystals: A “self-activated” configurational transition

Y. N. Chen,^{1,a)} S. J. Xu,^{1,b)} C. C. Zheng,^{1,c)} J. Q. Ning,¹ F. C. C. Ling,¹ W. Anwand,² G. Brauer,² and W. Skorupa³

¹Department of Physics, HKU-Shenzhen Institute of Research and Innovation (HKU-SIRI), HKU-CAS Joint Laboratory on New Materials, The University of Hong Kong, Pokfulam Road, Hong Kong, China

²Institute of Radiation Physics, Helmholtz-Zentrum Dresden-Rossendorf, Bautzner Landstr. 400, D-01328 Dresden, Germany

³Institute of Ion Beam Physics and Materials Research, Helmholtz-Zentrum Dresden-Rossendorf, Bautzner Landstr. 400, D-01328 Dresden, Germany

(Received 16 June 2014; accepted 20 July 2014; published online 1 August 2014)

By implanting Zn⁺ ions into research-grade intentionally undoped ZnO single crystal for facilitating Zn interstitials (Zn_i) and O vacancies (V_O) which is revealed by precise X-Ray diffraction rocking curves, we observe an apparent broad red luminescence band with a nearly perfect Gaussian lineshape. This red luminescence band has the zero phonon line at ~2.4 eV and shows distinctive lattice temperature dependence which is well interpreted with the configurational coordinate model. It also shows a low “kick out” thermal energy and small thermal quenching energy. A “self-activated” optical transition between a shallow donor and the defect center of Zn_i-V_O complex or V_{Zn}V_O di-vacancies is proposed to be responsible for the red luminescence band. Accompanied with the optical transition, large lattice relaxation simultaneously occurs around the center, as indicated by the generation of multiphonons. © 2014 AIP Publishing LLC.

[<http://dx.doi.org/10.1063/1.4892356>]

Recently, ZnO has re-attracted tremendous interest as a promising light emitting material due to its wide band gap of ~3.44 eV at cryogenic temperature and its large free exciton binding energy of 60 meV.^{1–5} In terms of emission wavelength, the luminescence of ZnO can coarsely be categorized into two groups: the near-band-edge exciton sharp lines in the ultraviolet spectral region and the broad color bands in the visible light region. For most of the sharp lines, they have been firmly identified to be originated from the radiative recombination of various impurity-bound excitons.⁶ However, for the color emission bands, their origins are still controversial.^{1,7,8} Green, yellow, and red luminescence bands are the commonly observed color emissions in ZnO. They are known to originate from some deep centers very early,⁹ but they may have different origins.¹⁰ Recently, Liu *et al.* reported the polarized photoluminescence (PL) spectra of ZnO single crystals and suggest that the defect-related deep band emission in the visible range is closely associated with the Zn and O vacancies.¹¹ In this Letter, we present an in-depth investigation on the red luminescent center in research grade ZnO single crystals both experimentally and theoretically. By implanting Zn ions into the intentionally undoped ZnO single crystal, we create a Zn rich condition under which the defect centers formed are either the excess Zn ions placed interstitially (Zn_i) or the O vacancies (V_O) arising from the incorporation of the extra Zn ions at normal sites. Directly after the Zn ion implantation, a noticeable red

luminescence band is observed and is well interpreted with the configurational coordinate (CC) model. The electronic transition energy of the red luminescent center is inclusively determined to be 2.4 eV, taking into account the simultaneous multiphonon emission. The nature of this center including their charge states is discussed by the aid of the recent theoretical results on different native point defects and their optical transitions in ZnO.

The starting samples studied in this work were one-side polished, intentionally undoped, pressurized melt-grown ZnO single crystals, grown along [0001] direction with c axis terminated by Zn, produced by Cermet, Inc. We measured the PL spectrum of the as-grown ZnO sample at 3.5 K and found the band-edge exciton emission to be at 3.3592 eV, in excellent agreement with the Cermet’s data. The intensity of the color emissions of the starting sample is four orders of magnitude lower than that of the near-band-edge excitonic emission. Therefore, these ZnO single crystals with relatively lower trace impurities provide a good starting point for investigating defects, especially native defects in ZnO.¹² For creating Zn-rich conditions, Zn⁺ ions were incorporated into the polished side of the ZnO crystal at 300 °C using ion implantation technique. The acceleration energy and fluence of Zn⁺ ions were 500 keV and 10¹⁴ cm⁻², respectively. Under these conditions, implanted Zn ions in ZnO have a concentration depth profile peaking at a depth of 210.0 nm from the implanted surface.¹³ In the subsequent PL measurements, the samples were mounted on the cold finger of a Janis closed cycle cryostat providing a varying temperature range of 3.5–330 K. The excitation source was the 325 nm line of a Kimmon He-Cd continuous wave laser with an output power of 40.0 mW. Emission signals were dispersed by a SPEX 750M monochromator and detected with a

^{a)}Present address: Laboratoire “Matériaux et Phénomènes Quantiques,” Université Paris Diderot-Paris 7, CNRS-UMR 7162, 75013 Paris, France.

^{b)}Author to whom correspondence should be addressed. Electronic mail: sjxu@hku.hk

^{c)}Present address: Mathematics and Physics Centre, Xi’an Jiaotong-Liverpool University, 111 Ren’ai Road, Suzhou 215123, China.

Hamamatsu R928 photomultiplier. Standard lock-in amplifier technique was employed. A long-pass filter LP38 was employed for measurements involving wavelengths beyond 650 nm. Thermal annealing processes were performed on the Zn-implanted samples, at 500 and 650 °C, respectively. For each temperature, the annealing process was performed for 30 min in Ar gas and optical investigation was performed after each process.

In ZnO, there usually has a strong electron-phonon coupling at deep centers. For example, the Huang-Rhys factor S characterizing electron-phonon coupling strength is as large as $S = 6.5$ for the frequently observed structured green emission band in ZnO.¹⁴ Such strong electron-phonon coupling results in a large redshift of spectral peak in PL spectrum with respect to the energy of the electronic level involved in the optical transition. One thus has to identify the zero-phonon line (ZPL) which gives the energetic location of the defect level involved in the emission process. To do so, we employ the underdamped multimode Brownian oscillator (MBO) model as previously done by us.¹⁴ The MBO model is a generalized model that takes into account both the coupling of electrons with the primary phonon mode (i.e., longitudinal optical phonon) and the dissipative effect of the secondary acoustic phonon bath for photon absorption and emission.¹⁵

In addition to the MBO model, we attempt to employ the CC model to examine the luminescent center for getting a deeper understanding. In fact, the CC model is very successful in the interpretation of various luminescent centers in different solids including wide band gap semiconductors,^{16,17} which has led to several important conclusions: (1) The luminescence is usually quite broad due to the simultaneous generation of many phonons and shows a nearly perfect Gaussian symmetric lineshape; (2) The line width W (i.e., the full width at the half maximum, FWHM) of the luminescence band varies with temperature according to the relation

$$W(T) = W_0 [\tan h(\hbar\omega/2k_B T)]^{-1/2}, \quad (1)$$

where W_0 is a temperature independent constant, $\hbar\omega$ is the characteristic energy of phonons involved in the emission, k_B is the Boltzmann constant, and T is the absolute temperature; (3) The spectral peak of the luminescence band shifts to the higher energy side with increasing temperature.¹⁷ If only one phonon mode is taken into account, the spectral peak $E(T)$ may blueshift linearly with increasing temperature

$$E(T) = E(0) + \alpha k_B T, \quad (2)$$

where $E(0)$ is the spectral peak at $T = 0$ K and α is a constant. Later, we show the application of the CC model to the case of the red luminescent center in ZnO after the Zn⁺ ion implantation.

In order to obtain the information of defect creation in ZnO lattice by Zn ion implantation, we have conducted measurements of fine X-ray diffraction (XRD) rocking curves on the as-grown and as-Zn-implanted ZnO.¹³ From the XRD rocking curves (not shown here), we can see that the ion implantation causes several satellite structures located on both sides of the main diffraction peak, indicating the formation of

defects and lattice distortion within several hundreds of nanometers.¹³ By adopting the kinematic model developed from the dynamical X-ray diffraction theory for uniform single crystal to fit the experimental XRD rocking curves, we can get the information of strain depth distribution along the implantation direction. In the as-Zn-implanted ZnO sample, the compressive and tensile strains are found to be simultaneously present. Moreover, the compressive strain distribution appears in the region near the implantation surface and then the tensile strain distribution successively appears.¹³ This means that vacancy-type defects are produced in the shallower regions while the interstitial defects are introduced in the deeper regions from the surface. It is known that the local strain in the ion-implanted region is usually induced by incorporation of implanted ions into host crystal. At the original lattice sites, substitutions or interstitials and or vacancy-interstitial pairs may be generated by the collision of the injected ions with atoms of the target.¹⁸ Therefore, the native point defects of Zn_i⁺ at interstitial sites and Zn⁺ at normal site + V_o⁻ vacancies should be introduced by the forced incorporation of Zn⁺ ion due to the charge compensation principle. This result provides a vital clue to the identification of luminescent center in ZnO after Zn ion implantation.

Figure 1 shows the measured 3.5 K color emission bands of the as-Zn-implanted ZnO (solid circles) and post-implantation ZnO thermally annealed at 500 (solid line + solid squares) and 650 °C (solid line + solid triangles). A noticeable red luminescence band peaking at ~ 626 nm is observed in the as-Zn-implanted sample. At the same time, a significant drop in intensity is seen for the near-band-edge luminescence (not shown here). As mentioned earlier, the MBO model is used to find out the ZPL position of the red luminescence band. A good fit is obtained, as shown in the solid line in Fig. 1, with the parameters used: the energy of the ZPL $E_{ZPL} = 2.398$ eV, $S = 6.5$, $\hbar\omega = 71.2$ meV, and the damping coefficient $\gamma = 150$. Therefore, the optical transition level of the luminescent center giving the broad red emission band in the as-Zn-implanted ZnO crystal has energy of 2.398 eV. Note that this red luminescence band is almost eliminated by 500 °C thermal annealing, meaning

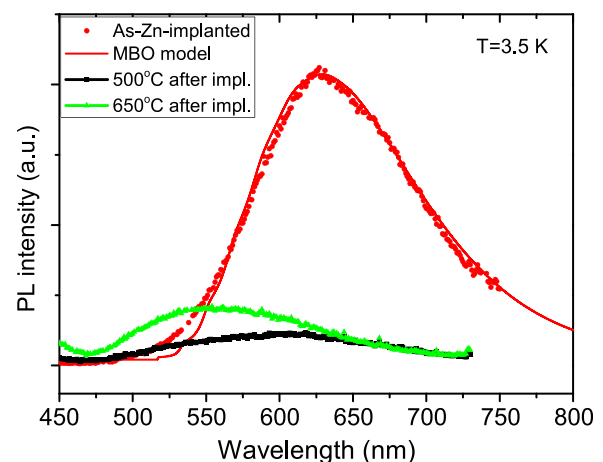


FIG. 1. The color emission spectra (symbols and lines + symbols) of the as-Zn-implanted ZnO sample and the same sample thermally annealed at the indicated temperatures in the Ar gas atmosphere. The solid line is the theoretical spectrum using the MBO model.

that the energy barrier of this luminescent center is less than 50 meV. This relatively low energy barrier suggests that the defect (or complex) possesses a small removal (dissociation) energy. Liu *et al.* also observed the lowest concentration of O vacancies related defects in their ZnO sample annealed at 400 °C in air.¹¹ Furthermore, the thermal treatment of the implanted sample at 650 °C causes the overall recovery of the near-band-edge luminescence (not shown here) and somewhat the activation of the green emission band.

Figure 2 shows the measured red luminescence band (thin lines + symbols) of the as-Zn-implanted ZnO at different temperatures. The three thick solid lines are the fits to the measured spectra at 4, 160, and 298 K with the Gaussian lineshape function. From Fig. 2, it can be seen that the red luminescence band remains a nearly perfect Gaussian lineshape at different temperatures, as described by the CC model. Other main spectral parameters, such as the spectral peak, line width, and integrated intensity, also show characteristic temperature dependence, as shown in Fig. 3. From the temperature evolution of these key spectral parameters, a dividing temperature point is observed at ~ 100 K. For example, starting from 3.5 K the spectral peak slowly blueshifts to reach a local maximum at around 40 K, and then slowly redshifts as the temperature increases. Beyond 100 K, the spectral peak blueshifts almost linearly, as shown in Fig. 3(a). The line width also shows an unusual small reduction with increasing temperature when less than 100 K, and exhibits a remarkable increase for temperature higher than 100 K, as seen in Fig. 3(b). The integrated intensity increases first and then drops exponentially when the temperature is beyond 100 K, which can be clearly seen in Fig. 3(c). The exponential reduction of the luminescence intensity with temperature indicates occurrence of thermal quenching. The activation energy ΔE for this thermal quenching process is determined to be 23 meV using the following equation:

$$I = C \exp(\Delta E/k_B T), \quad (3)$$

where I is the integrated luminescence intensity and C is a constant. This small thermal activation energy suggests that a shallow level may be involved in the red luminescence

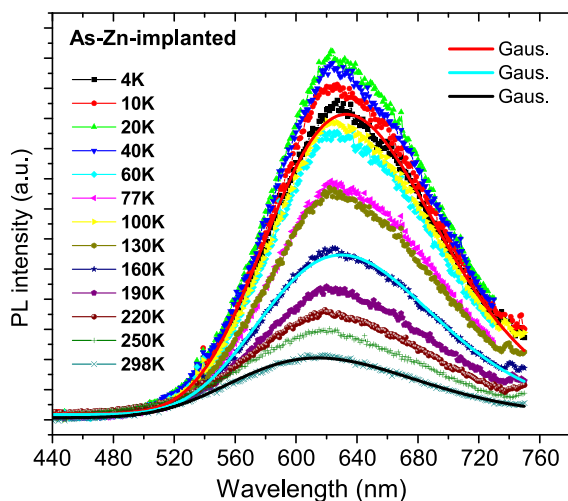


FIG. 2. The PL spectra measured of the as-Zn-implanted ZnO sample at different lattice temperatures. Three solid lines are the fitting curves using Gaussian lineshape function.

process. For the line width, its temperature dependence can be fitted quite well with the CC model (i.e., Eq. (1) described above) when $\hbar\omega = 71.2$ meV (i.e., the longitudinal optical phonon energy of ZnO) was adopted. The solid line is a linear fit with Eq. (1). The distinctive temperature evolution of the line width also obeys the CC model, as seen in Fig. 3(b). As for the spectral peak, once again, we see that its evolution with the lattice temperature basically follows the CC model's description. For example, the spectral peak blueshifts almost linearly with increasing temperature when the temperature is beyond 100 K, as shown in Fig. 3(a). The blueshift of the spectral peak caused by temperature elevation is mainly due to the thermal redistribution of electrons at the electron-vibration coupled states with higher energy.¹⁷ All these spectral characteristics and distinctive temperature dependence of the red luminescence band lead to the first assumption that it is originated from a kind of "self-activated" transition within a complex luminescent center in ZnO.

Actually, the "self-activated" luminescence has been previously observed in most of II-VI wide band gap semiconductors including ZnO and has been studied in detail for ZnS.¹⁹ For such a "self-activated" luminescent center, i.e., a shallow donor associated with a cation vacancy (i.e., V_{Zn}), its luminescence process is a cyclical process: the first excitation of an electron from the self-activated center to the conduction band of ZnS upon ultraviolet illumination changes the center to an ionized deep acceptor state called the A-center, then the electron was captured by the shallow donor of the center, and finally returns to the A-center via the luminescence process. However, the situation in ZnO is quite complicated.⁹ As already mentioned in the foregoing, the color luminescence bands in ZnO may have different origins.¹⁰ For the structureless green emission in ZnO, it could be from an associated V_{Zn} -impurity donor center like the blue luminescent center in ZnS.¹⁹ As for the red luminescence band in ZnO, nevertheless, we temporarily attribute it to another kind of "self-activated" center in terms of its luminescence characteristics and thermal treatment behaviors.

In ZnO crystals similar to the as-grown one studied in the present work, Zn and O di-vacancies ($V_{Zn}V_O$) were firmly detected using sensitive positron annihilation technique.²⁰ In the Zn-implanted sample, Zn_i and Zn_i-V_O complex are the two most possible native defects. The former causes somewhat extensile strain whereas the latter could result in some compressive strain as those revealed by our XRD data.¹³ In an early study of Zn doped ZnO, the native donor Zn_i , an unknown donor D, and the native acceptor V_{Zn} have been suggested as the major defects.²¹ Moreover, the unknown donor could be frozen-in oxygen vacancy V_O , which thermodynamically cannot be distinguished from a foreign donor.²¹ Therefore, Zn_i and Zn_i-V_O complex, as well as the original V_{Zn} should be the dominant native defects in the as-Zn-implanted ZnO. In, H, Ga, and Cu are the major trace impurities detected in the similar ZnO sample in term of their concentrations.¹² All these foreign impurities except Cu are well known to act as shallow donors in ZnO, while Cu is generally considered to be an acceptor.^{7,8} Recent theoretical calculations about the native defects as well as their transition levels among their different charge states based on the improved models have presented more precise results.^{22,23}

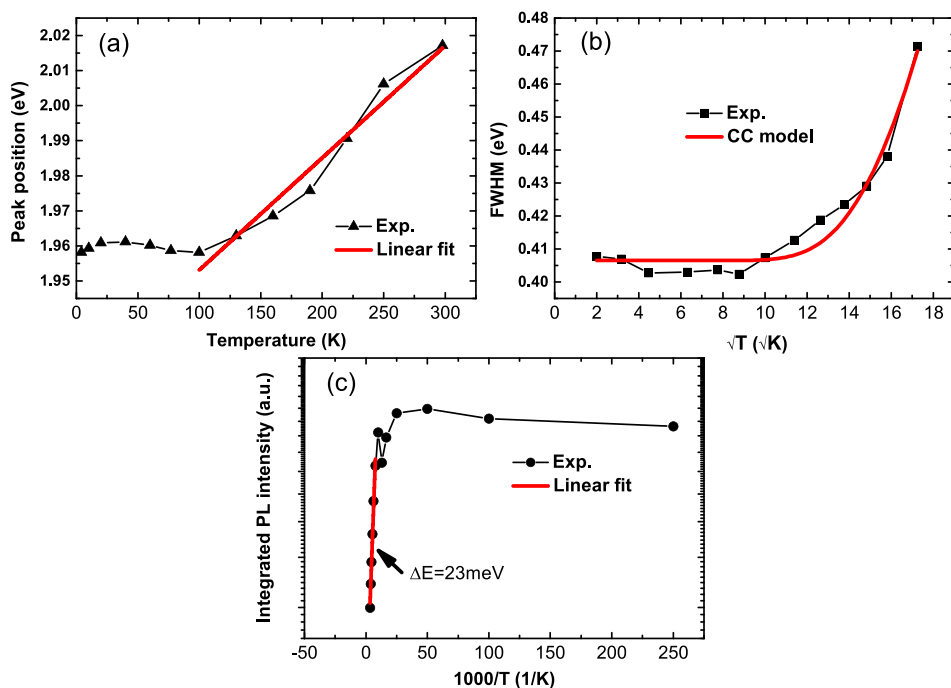


FIG. 3. Plots of the three spectral parameters: (a) the spectral center (peak position), (b) the line width (FWHM), and (c) the integrated intensity of the color emission band as a function of the sample lattice temperature for the as-Zn-implanted ZnO sample. The solid lines are the fitting curves.

Kim *et al.* found 1.97 and 2.53 eV transition levels within the $V_O\text{-Zn}_i$ defect complex which are close to our experimental value for the red luminescent center.²² Chakrabarty and Patterson obtained two transition levels of 2.5 and 2.4 eV within individual V_O and $V_{Zn}V_O$ defects, respectively, which are consistent with our experimental value for the red luminescent center. In particular, their theoretical value of the transition level between the -1 charge state to the neutral charge state of $V_{Zn}V_O$ is in excellent agreement with our experimental data.²³ From our experimental data and arguments, as well as by referring to the recent theoretical calculations, we would propose that the red luminescent center is a composite defect consisting of a native defect and an associated shallow donor. The $V_O\text{-Zn}_i$ defect complex and $V_{Zn}V_O$ di-vacancies are most likely to be the native defects involved in the red luminescence process.

In conclusion, a noticeable red luminescence band is observed in the research-grade undoped ZnO single crystals implanted with Zn ions. This red luminescence band has a ZPL of ~ 2.4 eV at cryogenic temperature and shows the spectral characteristics and distinctive temperature behavior of a kind of “self-activated” transition which can be well interpreted using the single coordinate CC model. A defect center containing a native defect complex and an associated shallow donor is proposed to be responsible for the red luminescence band. The most possible candidates for the involved native defect are the $V_O\text{-Zn}_i$ defect complex and the $V_{Zn}V_O$ di-vacancies rather than a simple point defect in ZnO.

This work was supported by the HK RGC-GRF (Grant No. HKU 703612P). One of the authors, S.J.X., wishes to thank Professor R. X. Wang for her helpful discussion. The financial support of the Hong Kong–Germany exchange service (DAA) with Grant No. G_HK026/07 is gratefully acknowledged.

- ¹Ü. Özgür, Ya. I. Alivov, C. Liu, A. Teke, M. A. Reshchikov, S. Doğan, V. Avrutin, S.-J. Cho, and H. Morkoç, *J. Appl. Phys.* **98**, 041301 (2005).
- ²*Zinc Oxide Bulk, Thin Films and Nanostructures: Processing, Properties and Applications*, edited by C. Jagadish and S. J. Pearton (Elsevier, 2006).
- ³*Oxide and Nitride Semiconductors*, edited by T. Yao and S.-K. Hong (Springer, Berlin Heidelberg, 2009).
- ⁴C. F. Klingshirn, B. K. Meyer, A. Waag, A. Hoffmann, and J. Geurts, *Zinc Oxide: From Fundamental Properties to Novel Applications* (Springer-Verlag, Berlin Heidelberg, 2010).
- ⁵J. W. Li, S. Z. Ma, X. J. Liu, Z. F. Zhou, and C. Q. Sun, *Chem. Rev.* **112**, 2833 (2012).
- ⁶B. K. Meyer, H. Alves, D. M. Hofmann, W. Kriegseis, D. Forster, F. Bertram, J. Christen, A. Hoffmann, M. Straßburg, M. Dworzak, U. Haboeck, and A. V. Rodina, *Phys. Status Solidi B* **241**, 231 (2004).
- ⁷M. D. McCluskey and S. J. Jokela, *J. Appl. Phys.* **106**, 071101 (2009).
- ⁸A. Janotti and C. G. Van de Walle, *Rep. Prog. Phys.* **72**, 126501 (2009).
- ⁹F. A. Cröger and H. J. Vink, *J. Chem. Phys.* **22**, 250 (1954).
- ¹⁰D. Li, Y. H. Leung, A. B. Djurišić, Z. T. Liu, M. H. Xie, S. L. Shi, S. J. Xu, and W. K. Chan, *Appl. Phys. Lett.* **85**, 1601 (2004).
- ¹¹J. Liu, Y. Zhao, Y. J. Jiang, C. M. Lee, Y. L. Liu, and G. G. Siu, *Appl. Phys. Lett.* **97**, 231907 (2010).
- ¹²G. Brauer, W. Anwand, D. Grambole, J. Grenzer, W. Skorupa, J. Čížek, J. Kuriplach, I. Procházka, C. C. Ling, C. K. So, D. Schulz, and D. Klimm, *Phys. Rev. B* **79**, 115212 (2009).
- ¹³C. C. Zheng, S. J. Xu, J. Q. Ning, Y. N. Chen, X. H. Lu, C. C. Ling, C. M. Che, G. Y. Gao, J. H. Hao, G. Brauer, and W. Anwand, *J. Appl. Phys.* **110**, 083102 (2011).
- ¹⁴S. L. Shi, G. Q. Li, S. J. Xu, Y. Zhao, and G. H. Chen, *J. Phys. Chem. B* **110**, 10475 (2006).
- ¹⁵S. Mukamel, *Principles of Nonlinear Optical Spectroscopy* (Oxford University Press, New York, 1995), p. 226.
- ¹⁶D. Curie, *Luminescence in Crystals* (Methuen and Co., Ltd., Great Britain, 1963), p. 31 and 50–51.
- ¹⁷S. Shionoya, *Luminescence of Inorganic Solids*, edited by P. Goldberg (Academic Press, Inc., New York, 1966), Chap. 4, p. 245.
- ¹⁸A. Pesek, *Appl. Phys. A* **58**, 141 (1994).
- ¹⁹B. C. Cavenett, *Luminescence Spectroscopy*, edited by M. D. Lumb (Academic Press, Inc., London, 1978), Chap. 5.
- ²⁰G. Brauer, W. Anwand, W. Skorupa, J. Kuriplach, O. Melikhova, J. Cizek, I. Procházka, C. Moisson, H. von Wenckstern, H. Schmidt, M. Lorenz, and M. Grundmann, *Superlattices Microstruct.* **42**, 259 (2007).
- ²¹K. I. Hagemark, *J. Solid State Chem.* **16**, 293 (1976).
- ²²D.-H. Kim, G.-W. Lee, and Y.-C. Kim, *Solid State Commun.* **152**, 1711 (2012).
- ²³A. Chakrabarty and C. H. Patterson, *J. Chem. Phys.* **137**, 054709 (2012).